

We are IntechOpen, the world's leading publisher of Open Access books Built by scientists, for scientists

6,900

Open access books available

185,000

International authors and editors

200M

Downloads

Our authors are among the

154

Countries delivered to

TOP 1%

most cited scientists

12.2%

Contributors from top 500 universities



WEB OF SCIENCE™

Selection of our books indexed in the Book Citation Index
in Web of Science™ Core Collection (BKCI)

Interested in publishing with us?
Contact book.department@intechopen.com

Numbers displayed above are based on latest data collected.
For more information visit www.intechopen.com



Analysis of Ultra-High Energy Muons at INO-ICAL Using Pair Meter Technique

Jaydip Singh, Srishti Nagu and Jyotsna Singh

Abstract

The proposed magnetized Iron CALorimeter (ICAL) detector at India-based Neutrino Observatory (INO) is a large-sized underground detector. ICAL is designed to reconstruct muon momentum using magnetic spectrometers as detectors. Muon energy measurements using magnets fail for high energy muons (TeV range), since the angular deflection of the muon in the magnetic field is negligible and the muon tracks become nearly straight. A new technique for measuring the energy of muons in the TeV range, used by the CCFR neutrino detector is known as the pair meter technique. This technique estimates muon energy by measuring the energy deposited by the muon in several layers of an iron calorimeter through e^+ and e^- pair production. In this work we have performed Geant4-based preliminary analysis for iron plates and have demonstrated the feasibility to detect very high energy muons (1–1000 TeV) at the underground ICAL detector operating as a pair meter. This wide range of energy spectrum will not only be helpful for studying the cosmic rays in the Knee region which is around 5 PeV in the cosmic ray spectra but also useful for understanding the atmospheric neutrino flux for the running and upcoming ultra-high energy atmospheric neutrino experiments.

Keywords: pair meter techniques, cosmic rays, iron calorimeter

1. Introduction

ICAL at INO is a 52 ktons detector [1] proposed to be built at Theni district of Tamil Nadu in Southern India. It is designed to study the flavor oscillations of atmospheric neutrinos. The main goal of the ICAL detector is to precisely measure the neutrino oscillation parameters and to determine the neutrino mass hierarchy [1]. At a depth of around 1.2 km underground, the INO-ICAL detector will be the world's biggest magnetized detector to measure cosmic ray muon flux with the capability to distinguish μ^+ from μ^- . The existing direct and indirect methods of muon spectrometry at accelerator-based and in cosmic rays (magnetic spectrometers and transition radiation detectors) experiments involve certain technical problems and limitations in the energy region $\geq 10^{13}$ eV. These disadvantages vanish in this alternate method where the muon energy is estimated by measuring the energy of secondary cascades formed by muons losing their energy in thick layers of matter, mainly due to the process of direct pair production of e^+ and e^- . By using this technique, muon energy can be estimated from INO-ICAL detector operating

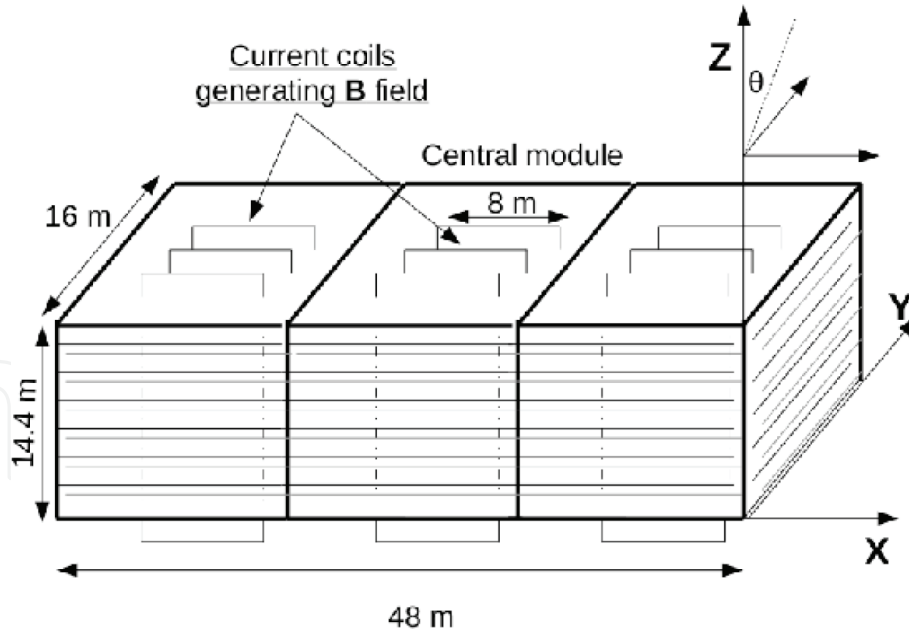


Figure 1.
Schematic view of three modules for the proposed INO-ICAL detector.

as a pair meter. The primary cosmic rays which are approximately in 50 TeV–50 PeV energy range correspond to this energy range [5].

This work presents a simulation based on the latest version of Geant4 [3] INO-ICAL code, developed by the INO collaboration for momentum reconstruction of muons in GeV energy range using INO-ICAL magnet. We have developed a separate Geant4 code for counting the muon bursts in iron plates for ultra-high energy muon analysis using the pair meter technique. The proposed detector will have a modular structure of total lateral size 48 m × 16 m, subdivided into three modules of size 16 m × 16 m. The height of the detector will be 14.5 m. It will consist of a stack of 151 horizontal layers of ~5.6 cm thick magnetized iron plates interleaved with 4 cm gaps to house the active detector layers. Detector geometry of ICAL magnet is presented in **Figure 1** and details of the components and dimensions are discussed in Ref. [1].

2. Momentum reconstruction analysis with ICAL magnet

In this section we have discussed the simulation for momentum reconstruction of muons in magnetic field. Details of the detector simulation for muons with energy of few 10's of GeV with older version of INO-ICAL code are already published in Ref. [4]. For simulating the response of high energy (100's of GeV) muons in the ICAL detector, 10,000 muons were propagated uniformly from a vertex randomly located inside 8 m × 8 m × 10 m volume. This is the central region of the central module where the magnetic field is uniform of 1.5 T. In our analysis we have considered only those events whose z coordinate of the input vertex lie within $z_{in} \leq 400$ cm which comprises the vertex to the central region. The input momentum and zenith angle are kept fixed in each case while the azimuthal angle is uniformly averaged over the entire range $-\pi \leq \phi \leq \pi$. In each case, we have studied the number of reconstructed tracks, the position resolution, including up/down discrimination and the zenith angle resolution. In this chapter, we have followed the same approach as in Ref. [4] for muon response analysis upto energy 500 GeV inside the detector [8]. Momentum reconstruction efficiency in the energy range of 1–400 GeV is shown in **Figure 2** and this energy range at the detector corresponds to the surface muon lying in the energy range 1600–2000 GeV from the top of the

surface. Muon will lose around 1600 GeV in the rock overburden [8] to reach at the detector from the top surface. Energetic muons from other directions will also hit the detector since the rock cover in other directions of detector is very huge, so we have not incorporated it in our discussion.

The momentum reconstruction efficiency (ϵ_{recon}) is defined as the ratio of the number of reconstructed events, n_{rec} , to the total number of generated events, N_{total} . We have

$$\epsilon_{recon} = \frac{n_{rec}}{N_{total}} \quad (1)$$

with error, $\delta\epsilon_{recon} = \sqrt{(\epsilon_{recon}(1 - \epsilon_{recon})/N_{total})}$.

Figure 2 shows the muon momentum reconstruction efficiency as a function of input momentum for different $\cos\theta$ bins, here left and right panels demonstrate detector response for low and high energy muon momentum respectively. One can see that the momentum reconstruction efficiency depends on the incident particle momentum, the angle of propagation and the strength of the magnetic field. As the input momentum increases, the reconstruction efficiency increases for all angles because with increase in energy the particle crosses more number of layers producing more hits in the detector. But at sufficiently high energies, the reconstruction efficiency starts decreasing, since the muons travel nearly straight without being deflected in the magnetic field of the detector. Track reconstruction is done using Kalman Filter techniques [4], tracks for few typical energies are plotted in **Figure 3**, which shows the deflected and undeflected muon tracks depending on the energy of muons in a fixed magnetic field (1.5 T).

Pair meter techniques:

1. High energy muons produce secondary cascades mainly due to electron pair production process.
2. It is one of the most important processes for muon interaction at TeV energies, pair creation cross section exceeds those of other muon interaction processes in a wide range of energy transfer:

$$100 \text{ MeV} \leq E_0 \leq 0.1E_\mu, E_0 \text{ is threshold energy.}$$

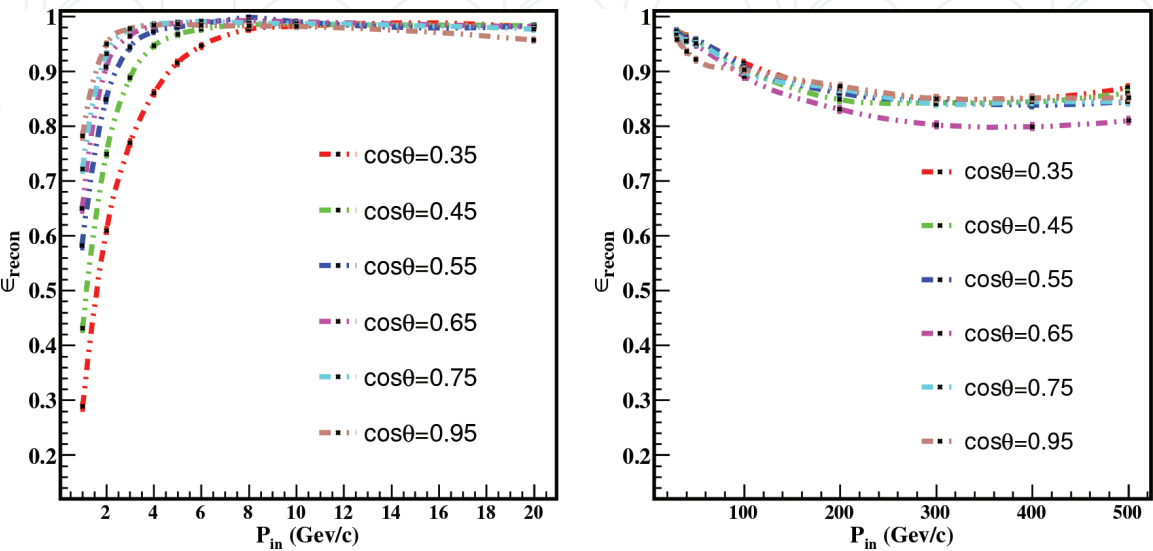


Figure 2. Reconstructed momentum efficiency as a function of the input momentum for different $\cos\theta$ values at low (1–20 GeV) and high energy (20–500 GeV).

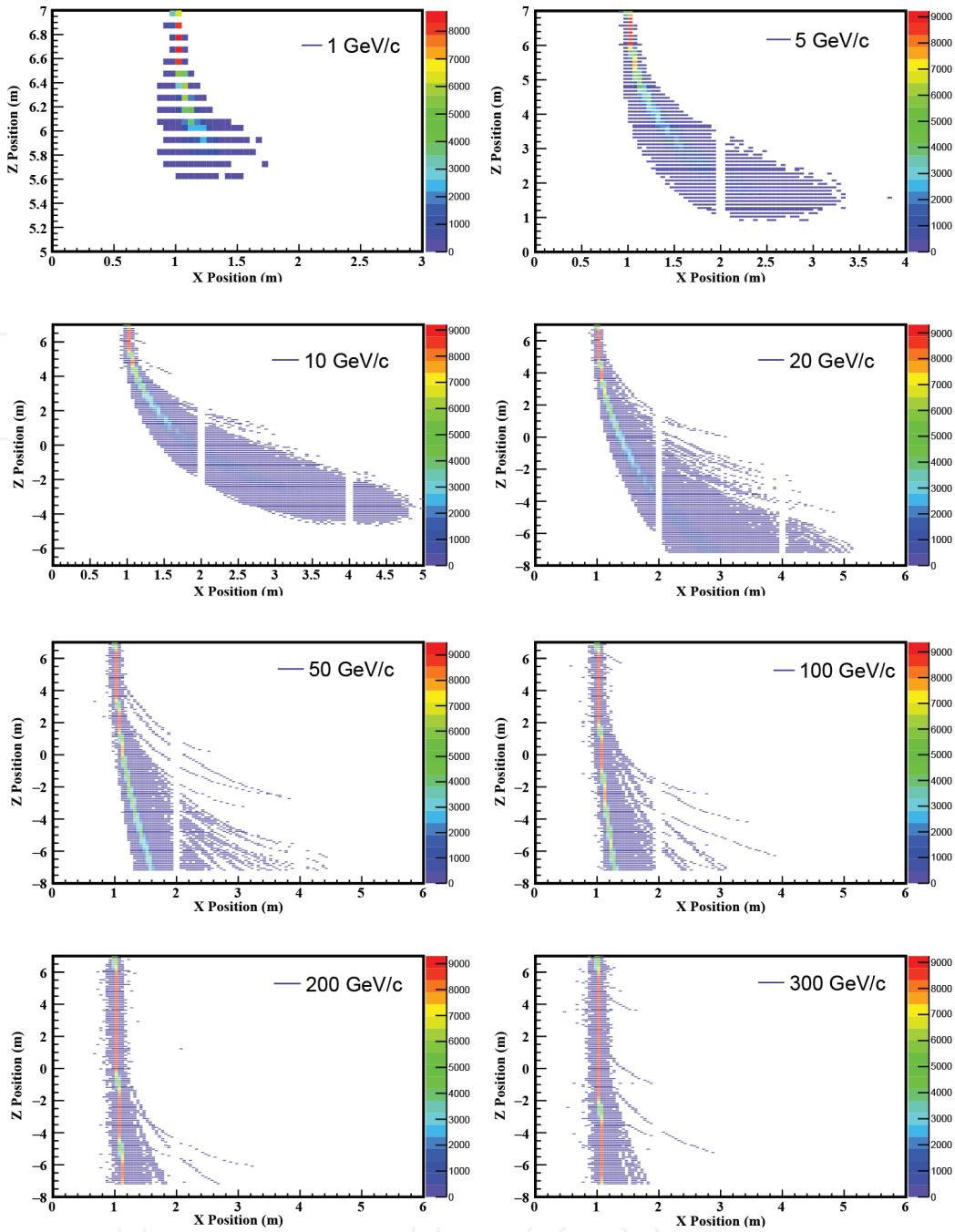


Figure 3.
Fixed energy muons track stored in X-Z plane of the detector going in the downward direction.

3. Average energy loss for pair production increases linearly with the increase in the muon energy and in the TeV region this process contributes more than 50% of the total energy loss rate.
4. Pair meter method for energy reconstruction of high energy muons has been used by the NuTeV/CCFR collaboration [6].

2.1 Average number of burst calculation

The e^+ and e^- pair production cross section by a muon of energy E_μ with energy transfer above a threshold E_0 increases as $\ln^2 (2m_e E_\mu / m_\mu E_0)$ where m_μ and m_e are the masses of the muon and the electron respectively [1]. Defining $v = E_0 / E_\mu$, above $v^{-1} = 10$, this cross section dominates over other processes by which the muon loses its energy when it passes through dense matter, generating observable cascades.

- The pair production cross section depends upon E_μ/E_0 which allows one to estimate the energy of muon by counting the number of interaction cascades M in the detector with energies above a threshold E_0 .
- Differential cross section for pair production is estimated in Ref. [1] and that expression is given by:

$$v \frac{d\sigma}{dv} \simeq \frac{14\alpha}{9\pi t_0} \ln \left(\frac{km_e E_\mu}{E_0 m_\mu} \right) \quad (2)$$

where $\alpha = 1/137$, $k \simeq 1.8$ and t_0 is the radiation length(r.l.) of the material, for iron $t_0 = 13.75 \text{ g/cm}^2$.

- The average number of interaction cascades M above a threshold E_0 is given by:

$$M(E_0, E_\mu) = T t_0 \sigma(E_0, E_\mu) \quad (3)$$

$$E_\mu = (E_0 m_\mu / km_e) \exp(\sqrt{9\pi M / 7\alpha T - A}) \quad (4)$$

where T is target thickness and $\sigma(E_0, E_\mu)$ is the integrated cross section(in unit of cm^2/g) and $A \simeq 1.4$.

$$\sigma(E_0, E_\mu) \simeq \frac{7\alpha}{9\pi t_0} \left(\ln^2 \left(\frac{km_e E_\mu}{E_0 m_\mu} \right) + A \right) \quad (5)$$

3. Counting the burst using pair meter

A muon traversing vertically from the top will cover $151 \times 5.6 \simeq 845 \text{ cm}$ in iron plates, this is equivalent to a path-length of $\simeq 480 \text{ r.l. (g/cm}^2\text{)}$. The number of cascades produced by high energy muon for a path length of $450 \text{ r.l. (g/cm}^2\text{)}$ can be calculated using Eq. (3). The number of cascades produced as a function of muon energy is shown in **Figure 4**, which increase with energy in the energy range 10^3 – 10^6 GeV (1–1000 TeV). One can interpret from **Figure 4** that the approximate number of interactions for a 1 TeV muon at threshold energy E_0 of 1 GeV is 4. Similarly for a 10 TeV muon, the number of interactions for $E_0 = 10 \text{ GeV}$ is 4 and for 1 GeV is 20. For a 100 TeV muon, the number of interactions for $E_0 = 100 \text{ GeV}$ is around 4, for $E_0 = 10 \text{ GeV}$ is close to 20 and for $E_0 = 1 \text{ GeV}$ is approximately 50.

3.1 Penetration depth of electron in the iron plates

The estimation of muon burst energy in iron plates is done by evaluating the energy of electron and positron pair, for that e^+ and e^- must hit the active elements of the detector, that is, the RPC which is a type of spark chamber with resistive electrodes placed parallel to each other. Measurement of penetration depth of the electron in iron gives us a handle to determine the energy loss of the electrons in the iron plates. The energy loss of electron in iron is given by: $E = E_0 e^{-x/x_0}$, where x is distance traveled in the iron plate and x_0 is the radiation length. It is thus important to determine the range of electron in iron plates which is shown in **Figure 5**.

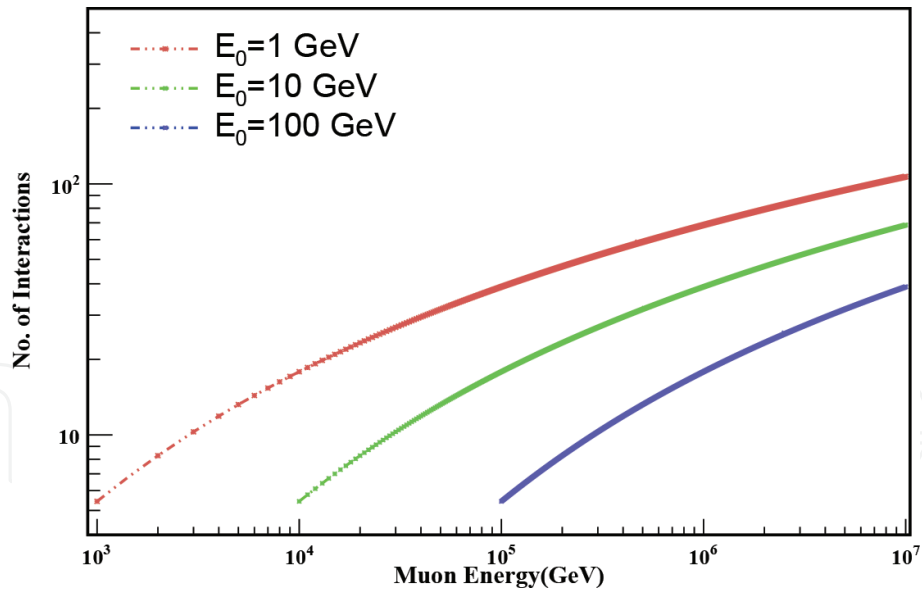


Figure 4. Average number of bursts above a threshold E_0 versus muon energy for $E_0 = 1, 10$ and 100 GeV, with T fixed to 450 r.l.

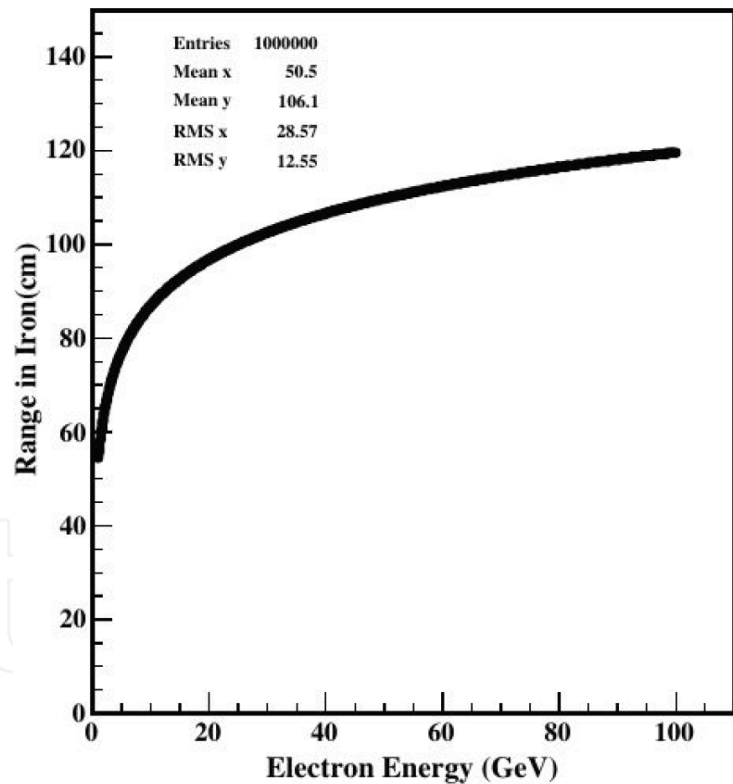


Figure 5. Energy of the electron and its corresponding penetrating range in the iron plates.

3.1.1 Muon burst of a few typical energies in the iron plates

A Geant4-based code is developed for simulating the muons burst in iron plates, here horizontal axis is the z -axis of INO-ICAL detector, in which 152 layers of iron plates of width 5.6 cm are placed vertically, interleaved with 2.5 cm gaps for placing the RPC. Muons are propagated using Geant4 particle generator class and generated bursts in the iron plates are counted, muon bursts for a $10, 100, 500$ and 1000 GeV are shown in **Figure 6(a)–(d)** respectively [7].

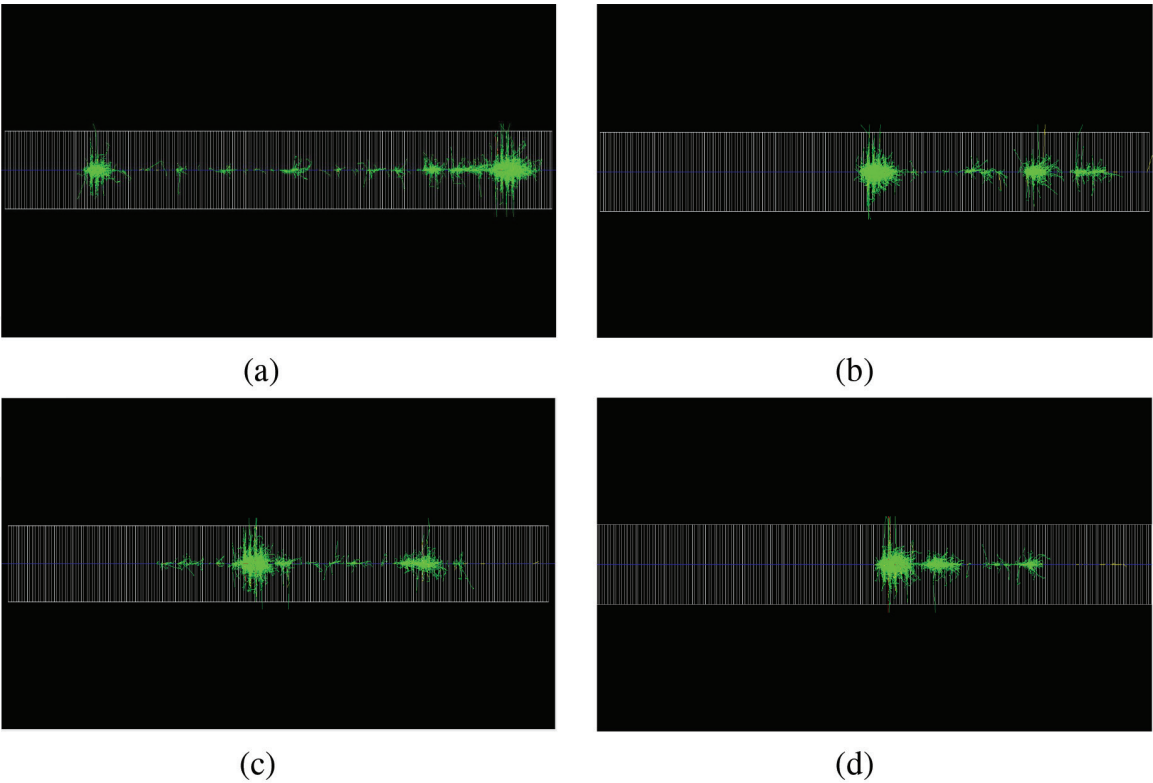


Figure 6.
Cascade generation for a few typical energies. Blue line (muon) represents z-axis of the detector and green line represents the electron-positron cascade in the x-y plane.

3.2 Operating ICAL using pair meter technique

Cosmic rays are composed of highly energetic particles mostly protons, alpha particles and a small fraction of heavier nuclei that reach the Earth from the outer space. Supernova bursts, quasars and other astronomical events are believed to be the sources of cosmic rays ranging over 10^{20} eV of energy [9]. The cosmic ray (CR) spectrum depicts a power law behavior over the entire spectral range but displaying two transition regions where the slope of the spectrum changes abruptly. The

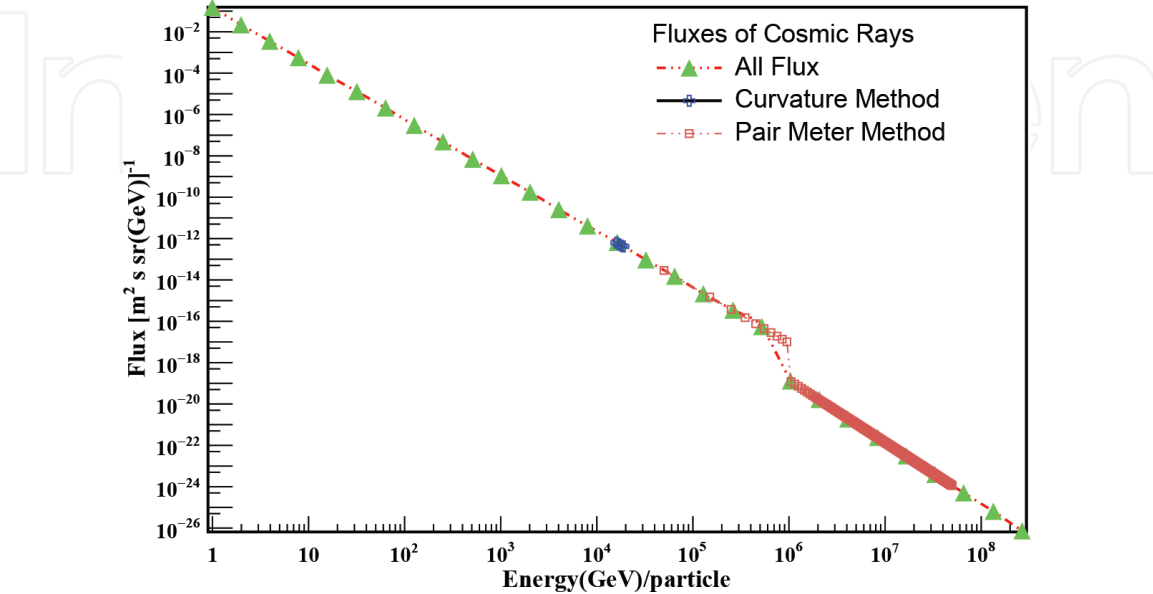


Figure 7.
Primary cosmic ray flux ($\phi \simeq KE^{-\alpha}$, where $\alpha \simeq 2.7$ and for KNEE (3PeV) $\alpha: 2.7 \rightarrow 3$) versus energy of primary particle, and limited range for ICAL to cover the spectrum using magnetic field and pair meter technique.

region around $E \sim 5$ PeV is where the CR spectrum becomes steeper, is known as the ‘knee’ region. At higher energy around $E \sim 5000$ PeV, the CR spectrum flattens at the ‘ankle’ where the sources of such high energies are believed to be of extra-galactic origin. The reason for these two appreciable ‘breaks’ in the CR spectrum is still unknown. Once accelerated at supernova shocks, cosmic rays have to propagate through the interstellar medium before they can be detected. CR muons are created when cosmic rays enter the Earth’s atmosphere where they eventually collide with air molecules and decay into pions. The charged pions (π^+ and π^-) decay in flight. All these particles together create into muons (μ^+ and μ^-) and neutrinos (ν and $\bar{\nu}$). A cascade called an air shower. Measurement of air shower particles can be interpreted in terms of the energy spectrum and primary cosmic ray composition. To determine these measurements we require calculation of fluxes generated via CR nuclei of mass A , charge Z and energy E .

Figure 7 represents primary cosmic ray flux versus energy of the primary cosmic ray particle. From **Figure 7**, we can see the limit of the energy range upto which magnetic spectrometers work i.e. around $E \sim 10^4$ while the pair meter technique works well in a wide energy range from 5×10^4 – 5×10^7 GeV.

4. Results and discussion

In Section 2, we have discussed the limitation of magnetized ICAL detector to be used as a magnetic spectrometer, which limits the efficiency of the detector to discriminate between μ^+ and μ^- at higher energies and reconstruct momentum. Variation in efficiency of muon momentum reconstruction as a function of input momentum is shown in **Figure 2**, which shows a clear fall in efficiency for energetic muons. In **Figure 3**, muon track could be seen, which is undeflected for highly energetic muons. Finally, it is concluded that with ICAL detector we can do analysis for muons in the energy range of 1–400 GeV. This corresponds to surface muons in the energy range of 1600–2000 GeV, because muons lose around 1600 GeV energy [3] into the rock overburden to reach at the detector from the top of the INO-ICAL surface. ICAL cannot be used as a magnetic spectrometer for highly energetic cosmic ray muons. For energetic (TeV) muons, pair meter technique [2] can be used for momentum reconstruction as discussed in Section 3 [5]. This technique is tested by a few detectors, since INO-ICAL will be large in dimensions so it will be a perfect machine to test the capability of this technique. We have developed a separate Geant4 code for counting the bursts in the iron plates and also a technique to measure the energy of the bursts with the produced electron pairs into the iron plates. In **Figure 6**, we can see the burst of muons in iron plate. The variation of these burst number is shown in **Figure 4**, which is a function of the muon energy.

4.1 Summary and conclusions

- The pair meter technique can competently measure muon energy in the energy range of 1–1000 TeV at INO-ICAL detector operating as pair meter.
- One can probe very high energy muon fluxes and primary cosmic rays in the knee region which will aid in accurate background muon and neutrino flux measurement in the forthcoming detectors designed for ultra-high energy neutrino experiments.
- Our Geant4 analyses for central module of INO-ICAL detector are successfully performed and variation in the cascade number of varying energy is observed in the iron plates.

Acknowledgements

This work is partially supported by Department of Physics, Lucknow University, Department of Atomic Energy, Harish-Chandra Research Institute, Allahabad and INO collaboration. Financially it is supported by government of India, DST project no-SR/MF/PS02/2013, Department of Physics, Lucknow University. We thank Prof. Raj Gandhi for useful discussion and providing hospitality to work in HRI, Dr. Jyotsna Singh for her support and guidance in completing this work from Lucknow University.

Author details

Jaydip Singh*, Srishti Nagu and Jyotsna Singh
University of Lucknow, Lucknow, India

*Address all correspondence to: jaydip.singh@gmail.com

IntechOpen

© 2018 The Author(s). Licensee IntechOpen. This chapter is distributed under the terms of the Creative Commons Attribution License (<http://creativecommons.org/licenses/by/3.0>), which permits unrestricted use, distribution, and reproduction in any medium, provided the original work is properly cited. 

References

- [1] Ahamed S, Sajjad Atahar M, et al. (INO Collab). Physics potential of the ICAL detector at the Indian based neutrino observatory. 9 May 2017; arXiv:1505.07380
- [2] Kokoulin RP, Petrukhin AA. Theory of the pairmeter for high energy muon measurements. *Nuclear Instruments and Methods in Physics Research*. 1987;**A263**(1988):468-479
- [3] Groom DE, Mokhov NV, Striganov S. Muon stopping power and range tables 10 MeV-100 TeV. *Atomic Data and Nuclear Data Tables*. 2001;**76**(2)
- [4] Chatterjee A et al. (INO Collab). JINST 9(2014) PO 7001; July 2014
- [5] Gandhi R, Panda S. Probing very high energy prompt muon and neutrino fluxes and the cosmic ray knee via underground muons. 31 August 2006; arXiv:hep-ph/0512179
- [6] Chikkatur AP, Bugel L, et al. Test of a calorimetric technique for measuring the energy of cosmic ray muon in TeV energy range. *Zeitschrift für Physik*. 1997;**74**:279-289
- [7] Agostinelli S et al. GEANT4: A simulation toolkit, GEANT4 collaboration. *Nuclear Instruments and Methods in Physics Research Section A*. 2003;**506**:250 <http://geant4.cern.ch/>
- [8] Singh J, Singh J, et al. Atmospheric muons charge ratio analysis at the INO-ICAL detector. 29 Jun 2018; arXiv:1709.01064
- [9] Ramesh N, Hawron M, Martin C, Bachri A. Flux variation of cosmic muons. *Journal of the Arkansas Academy of Science*. 2011;**65**:67-72